SS-map
Visualizing cooperative secondary structure elements in protein ensembles

Jelisa Iglesias, Melchor Sanchez-Martínez, and Ramon Crehuet*

Institute of Advanced Chemistry of Catalunya; CSIC; Barcelona, Spain

We present SS-map, a tool to visualize the secondary structure content of ensembles of proteins. When generating ensembles of intrinsically disordered proteins, we lose the understanding a single native structure gives for folded proteins. It then becomes difficult to visualize the composition of the ensembles or to detect transient helices such as MoRFs. Conformational propensities for single residues also hide the nature of cooperative structures. Here we show how SS-map describes folded and unfolded ensembles of some peptides and gives a new view of the ensembles used to describe intrinsically disordered proteins with residual structure in computational and NMR experiments. This tool is implemented in an open-source python code located at code.google.com/p/ss-map

Intrinsically Disordered Proteins (IDPs) exist in solution as ensembles of structures. This raises a challenge to us, humans, as we tend to understand structures by visualizing them,[1] and we lack ways to represent ensembles. Ensembles contain structural information, even when IDPs satisfy random-coil statistics.[2,3] Some regions of IDPs can adopt secondary structures, at least for a transient time.[4] This can be probed with experimental techniques such as NMR, in particular with Residual Dipolar Couplings (RDCs).[5-8] Structured regions, termed MoRFs, are key to recognition processes mediated by coupled folding-binding events.[9] The interpretation of data derived from NMR is usually done by stating that a certain segment of the protein chain adopts a certain secondary structure in a percentage of the total ensemble, but this conveys information in a difficult way for scientists not familiar with these interpretations. How can the ensembles be represented to better unveil their structure?

When studying protein folding, ensembles coming from computations are represented along the reaction coordinate of native contacts. This shows that for many (small) proteins, folding is a 2-state process. Thus, it is a cooperative event where most of the ensemble at a given temperature is either folded or unfolded. Victor Muñoz has pioneered the study of downhill folders, which fold in a progressive manner.[10] How do MoRFs of IDPs behave? Contact order discriminates between 2-state and downhill folders, but it cannot be used in IDPs because it is based on the concept of a well-defined native structure. MoRFs are usually described as the ratio of residues that adopt a certain secondary structure. It is important to differentiate when residues in a fragment independently adopt a conformation in a secondary structure region, from when that fragment contains a true secondary structure, with all the residues adopting that conformation at the same time, even if that structure is only adopted rarely. Indeed, if n residues are in an α-helical region 20% of the time, that does not mean an helix of n residues is present 20% of the time. Whether this happens or not will lead to different experimental results, such as different RDCs, and it would be desirable to visualize the structural differences of these ensembles.

In this communication we present a way to represent the cooperativity or the correlations in secondary structure formation for IDPs, where the use of contact orders or native contacts is impossible. We named our approach SS-map, from Secondary Structure map. We first study 2-folded proteins near its melting temperature to link our SS-map with other visualization techniques used in the protein folding community. Then, we visualize an ensemble of a MoRF from a measles[11] and a Sendai[5,12] virus nucleoprotein. Finally we reconsider the existence of the polyproline II helix in IDPs.

The SS-map tool is available for download in http://code.google.com/p/ss-map/, under the GNU GPL v3 license. Graphical output from the SS-map is produced with the
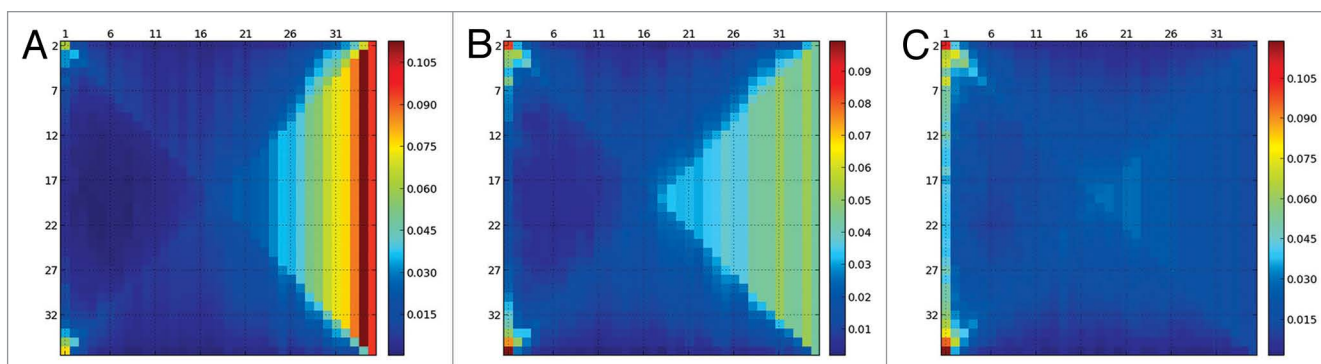
Figure 1. SS-map representing α-helices for the HPLC-6 peptide at different temperatures [(**A**): 313K, (**B**): 320K, (**C**): 327K)]. Large helices are lost below the melting temperature of 323K and all fragments grow from a central residue. At 320K an ensemble of helices with a wide range of lengths is present but shorter helices are not more abundant than longer ones.
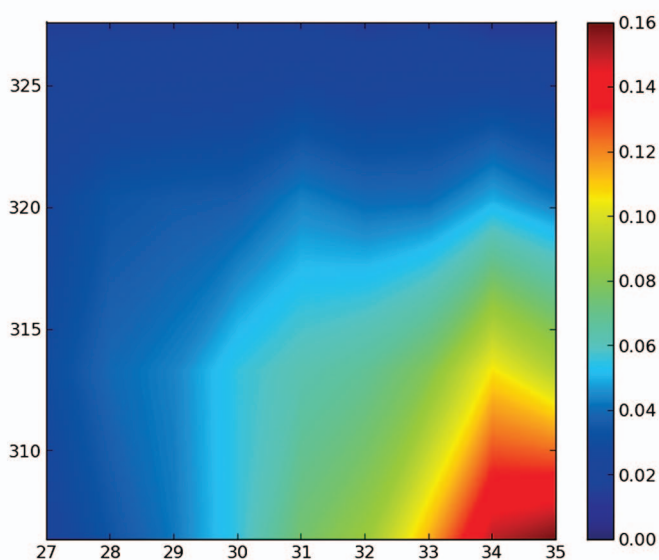

Figure 2. Temperature dependence of the presence of secondary structure elements at different temperatures. The x-axis represents the length of a helix element, and the y-axis the temperature. It shows how long helices are present only at low temperatures, and that helices do not get shorter, they just become much scarcer at higher temperatures (only the region of long helices is plotted, as the remaining region is essentially zero)

matplotlib library.[13] Details of the simulated ensembles are reported in the **Supplemental Material**.

The visualization tool presented in this work extends the calculation of secondary-structure percentage per residue one more dimension: we calculate and show the frequency of having n exactly contiguous residues in a certain secondary structure. For a protein with N+2 residues, this generates a matrix of NxN, where an element (m,n) corresponds to the frequency of having residue m forming a secondary structure element of length exactly n (see for example **Fig. 1**). Frequencies are normalized, so that if one wants the probability of residue m forming an helix of at least 4 residues, one can get it by summing row m, elements 4 to N.

There are different definitions of secondary structure elements. Currently our code can use the definition reported in reference 14, where all the Ramachandran space is assigned to an element; a more restrictive definition as in reference 15; or a user defined rectangular region of the Ramachandran plot. When the ensemble is input as a set of PDB files, SS-map uses the Bio.PDB[16] module of Biopython[17] to generate dihedral angles. Alternatively, we can use the external code Stride[18] to read the secondary structure. Differences in applying these definitions will be discussed below. A schematic workflow with the different possible input and outputs of SS-map is depicted in **Figure S1**.

The information that SS-map presents requires an image for each of the ensembles. This information can be compressed in 2 ways to represent several ensembles in one image. The raw-average gives the widely used probability of a certain residue being in the selected conformation, as **Figure S2** shows. The column-average gives new and complementary information: the percentage of fragments of a given length. This information can then be combined for different ensembles, for example, at different temperatures, such as in **Figures 2 and 3C**.

We first present a study of the unfolding of the peptide HPLC-6, which forms an α-helix and has a melting temperature of 323K when simulated with the Profasi force field.[19] The percentage of α-helix conformation for each peptide gradually decreases with temperature. This is more prominent at the N- and the C-terminus (**Fig. S2; Fig. S3**). The SS-map shows that at 313K a long helix spanning most of the residues is the most abundant structure (see **Fig. 1**). At 320K, this long helix is lost and fragments of different sizes are almost equally present, but in all cases, these fragments grow from the central residue 19. A representation of secondary structure per residue (**Fig. S2**) suggests that helices get shorter with temperature. This is not true: Long α-helix segments are not less frequent than shorter ones. At 320K, all fragments are rare, and the cumulative percentage of helices larger than 20 residues represents only a 21%. This number, at 313K is of 71%. At 327K, although the overall percentage of α-helix is still 45% (**Fig. S2**), there is no helix as such, only residues that adopt this conformation independently, without any cooperativity. This information cannot be reflected with the visualizations traditionally used, such as **Figure S2**, but it is
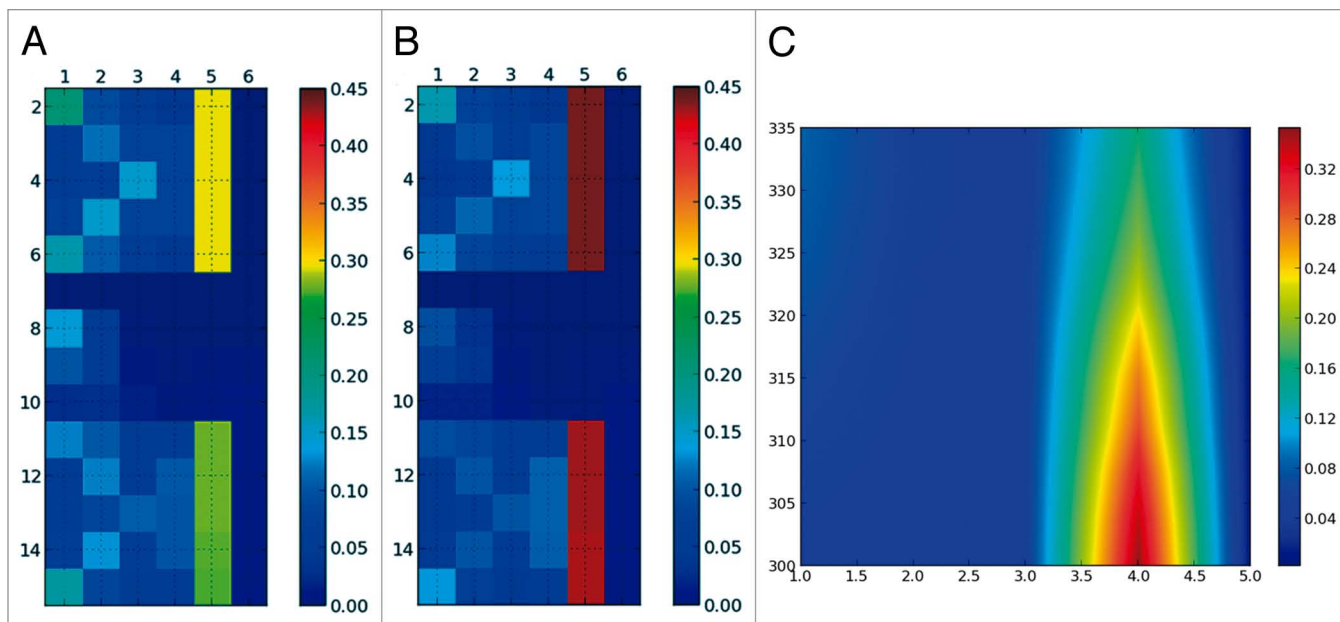
Figure 3. SS-map showing β-strands for the GB1p β-hairpin below the folding temperature [(**A**): 319K and above (**B**): 327K]. The temperature dependence of the SS-map shows that at all temperatures the most frequent strand has 4 residues (**C**).

relevant to interpret the results of circular dicroism that revealed a non-negligible percentage of α-helix even at 343K:[20] our interpretation is that it was only due to isolated residues in α-helix, and not to true helical segments.

The information of a range of ensembles at different temperatures can be compressed as previously explained. **Figure 2** shows that the long helix spanning 34 or 35 residues is lost between 310 and 315K, and then the ensemble is composed of helices of several different lengths. An essentially unfolded ensemble at the melting temperature agrees with recent similar findings for the more complex Protein A.[21]

We now focus on a structure that forms a β-hairpin, i.e., 2 β-sheets connected by a turn. We have taken a mutated from of the GB1p peptide (GB1m2)[22] also studied with the Profasi force field.[19] The simulated melting temperature for this peptide is very similar to the previous α-helix, 324K. The SS-map shows 2 β-strands and an empty 4-residue central region, which corresponds to the β-turn (**Fig. 3**). Even above the transition temperature, the strands of the hairpin remain the most populated structures, in contrast to the α-helix. The SS-map shows that the unfolded state of this β-hairpin—ensembles above the folding temperature—has different structural characteristics than the unfolded state of the α-helix (**Fig. 1**; **Fig. 2**). The temperature profile of the SS-map in **Figure 3** also contrasts with the one for the α-helix.

We now focus on a true IDP that contains fragments of partial secondary structure. These fragments are called MoRFs and correspond to binding regions of the IDPs.[9] Partially ordered regions are a challenge for many biophysical techniques,[4] but a successful approach is the use of NMR Residual Dipolar Couplings.[6-8] Here we will consider 2 proteins: a Measles virus nucleocapsid protein[11] and a Sendai virus nucleoprotein,[5] both studied by Blackledge and coworkers. In both proteins, the authors used a random-coil model

named Flexible Meccano[12,23] to generate an ensemble of structures (**Fig. 4**). Then they added helical fragments—in a statistically robust way—until they achieved a satisfactory fit of the RDCs. A special conformational treatment was given to the N-capping residues of the helices. The N-capping modifications are not implemented in the public version of Flexible Meccano, and therefore our ensembles differ from the ones used by Blackledge and colleagues (see the SI for a further discussion of this point). **Table 1** describes the composition of both ensembles.

The analysis of the ensemble using SS-map shows that the picture is more complex than it might seem. For example, helix H1 and H2 in the measles virus protein mix together to give an ensemble of helices that have lengths from 5 to 8 residues. Similarly helices H2 and H3 in the Sendai virus protein cannot really be differentiated and extend from the limits stated in **Table 1**. In our ensembles helices extend both toward the N-terminal and the C-terminal sense symmetrically, due to the lack of the N-capping treatment.

SS-map helps to bring light to these features, but as a visualization tool it does not substitute the work to determine what constitutes a correct ensemble. Here we have exploited the statistically sound analysis of Blackledge and coworkers to optimize the ensemble to fit the experimental data and we have only considered their best results.

The presence of polyproline II (PPII) helices in IDPs has been studied in several works. It has been related to the unexpected temperature behavior of IDPs[24] and its content correlates with the net charge of the IDPs[15] because PPII helices are the most stable conformations for charged residues.[25] We have analyzed the simulated ensembles of 4 IDPs studied by Pappu and colleagues, but here we only report the results for a poly-glutamine of 34 residues (id. 21 in their work[15]) because the results are similar for the other IDPs. Among all their reported IDPs, this one has the highest PPII
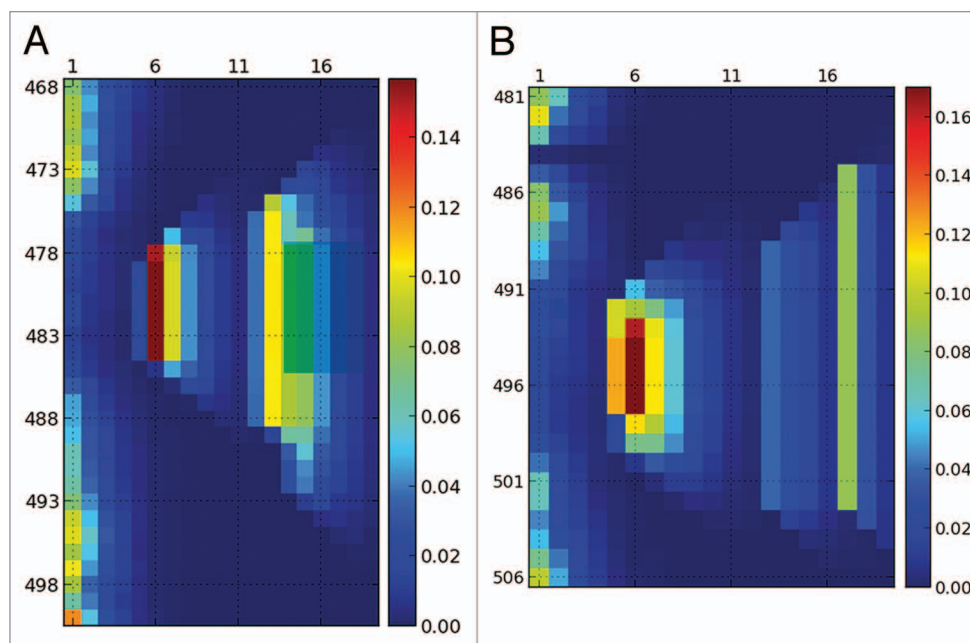
Figure 4. Helical content for the ensembles that reproduces the experimental RDCs of the Sendai virus nucleoprotein[5] (**A**) and the measles virus nucleoprotein[11] (**B**). Both ensembles were generated with Flexible Meccano by mixing ensembles with pre-defined helical content as detained in **Table 1**. Although 3 helices were used for the Sendai protein and 4 for the measles protein, the resulting ensemble is more continuous and mixed than **Table 1** might suggest.
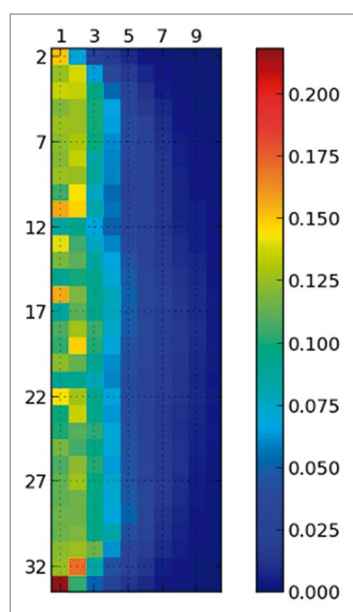

Figure 5. Content of Polyproline II for the 34-residue poly-glutamine, the region defining the polyproline II is the same as in the original study.[15] Although the natural propensity of all the residues is to be in PPII with a relevant frequency, the formation of a helix is not a cooperative process and long helices are absent, in contrast to the α-helices of **Figure 1**.

Table 1. Composition of the ensembles generated with Flexible Meccano[12,23] to reproduce the RDCs for the Sendai virus nucleoprotein[5] and measles virus nucleoprotein,[11] based on the data provided therein

	Residues	**Population (%)**
Sendai		
H1	479–484	36
H2	476–488	28
H3	478–492	11
Random coil	468–500	25
Measles		
H1	494–499	22
H2	492–497	30
H3	489–502	10
H4	485–502	13
Random coil	481–506	25

Remark that the N-capping aminoacids had a special conformational behavior not implemented in the public version of the Flexible Meccano code, and therefore the ensembles reported here differ from those described in the original references.[5,11]

content, as expected from its highest charge. Although the total PPII content is 51%, **Figure 5** shows that the longest helices present in the ensembles contain only 5 consecutive residues. To avoid being deceived by single-residue propensities, Pappu and coworkers counted only fragments of 3 or more consecutive residues in PPII conformation. SS-map removes the arbitrariness of that number "3" and conveys more information. As opposed to the α-helix in **Figure 1**, there is no growing helix from any central residue. Thus, long helices of PPII do not cooperatively form in solution, at least in the models used by Pappu and coworkers.[15] Considering that
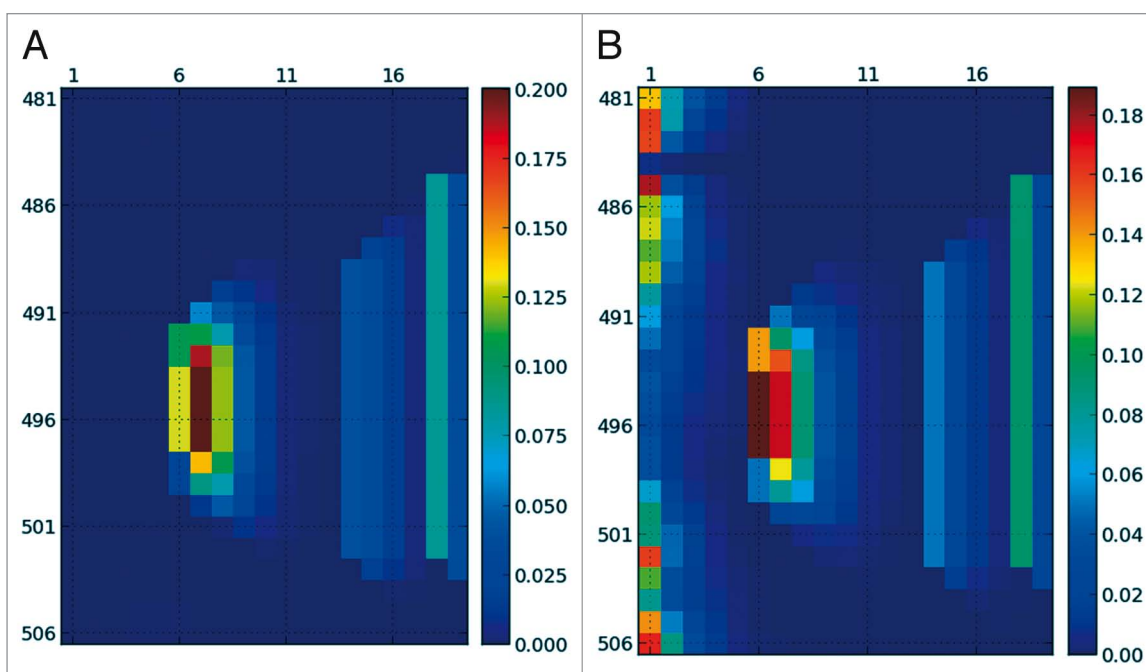
Figure 6. SS-map for the measles virus nucleoprotein showed in **Figure 4** using 2 different criteria to define the α-helix. The external program Stride (**A**), which only considers a secondary structure element when it is larger than 4 residues, and the definition used in reference 15 (**B**), which is approximately circular and much smaller than the region used by Blackledge and coworkers.[14]

electrostatic interactions in water increase with temperature,[26] it would be interesting to study how these ensembles change when heated. We leave that for future work.

Although everybody agrees on the qualitative description of α-helices and β-sheets, different groups partition the Ramachandran plot in different regions. For example, Blackledge and coworkers use big rectangular regions so that any point belongs to a given secondary structure.[14] Although these regions are larger than what is usually accepted, they allow the classification of all points in the Ramachandran plot. Pappu and colleagues use much more restrictive secondary structure elements,[15] closer to more wide-spread definitions such as the one in the Wikipedia.[27] In SS-map users can also measure with their own definitions. The effect of these arbitrariness could be more important in IDPs than in folded proteins, due precisely to their higher disorder. **Figure 6** shows the ensembles plotted using different criteria. It is interesting that the Stride program never considers a fragments of less than 4 residues to have a secondary structure, to model as closely as possible how crystallographers represent α-helices and β-strands.[18] Therefore, the results differ in those 1 to 3 residue fragments, but agree almost quantitatively in the rest. The more restrictive definitions used by Pappu and coworkers[15] lead to overall lower percentages of secondary structure fragments as expected, but the general picture remains the same (compare **Fig. 6** with **Fig. 4B**). Whether a consensus is necessary or not is something the scientific community has to decide, but our present findings suggest that the structural interpretations do not change significantly with varying definitions.

Understanding IDPs with partially folded regions is a challenge to both computation and experiment.[4] Conformations cannot be referenced or compared with a native structure and we need new tools to visualize these heterogeneous ensembles. In this work we presented a tool, SS-map, which literally adds a new dimension to the representation of IDPs ensembles. By including the correlation between secondary structure elements in fragments, a more detailed picture emerges. Differences between α-helices, β-strands and PPII regions become more evident. The ensembles used to reproduces RDCs data can also be visualized and compared. SS-map does not optimize or change the ensembles whatsoever, it only extracts information from them and displays it. The results are as realistic as the underlying ensemble is; finding these ensembles remains a challenge.[28] Finally, this tool can also be useful to analyze the folding process of small proteins and peptides.[29]

Supplemental Material

Supplemental material may be found here:
http://www.landesbioscience.com/journals/idp/article/25323/

References

1. Gan J, Norman C. 2012 Visualization Challenge. Science 2013; 339:509; http://dx.doi.org/10.1126/science.339.6119.509

2. Fitzkee NC, Rose GD. Reassessing random-coil statistics in unfolded proteins. Proc Natl Acad Sci U S A 2004; 101:12497-502; PMID:15314216; http://dx.doi.org/10.1073/pnas.0404236101

3. Jha AK, Colubri A, Freed KF, Sosnick TR. Statistical coil model of the unfolded state: resolving the reconciliation problem. Proc Natl Acad Sci U S A 2005; 102:13099-104; PMID:16131545; http://dx.doi.org/10.1073/pnas.0506078102

4. Dyson HJ. Expanding the proteome: disordered and alternatively folded proteins. Q Rev Biophys 2011; 44:467-518; PMID:21729349; http://dx.doi.org/10.1017/S0033583511000060

5. Jensen MR, Houben K, Lescop E, Blanchard L, Ruigrok RWH, Blackledge M. Quantitative conformational analysis of partially folded proteins from residual dipolar couplings: application to the molecular recognition element of Sendai virus nucleoprotein. J Am Chem Soc 2008; 130:8055-61; PMID:18507376; http://dx.doi.org/10.1021/ja801332d

6. Schneider R, Huang JR, Yao M, Communie G, Ozenne V, Mollica L, et al. Towards a robust description of intrinsic protein disorder using nuclear magnetic resonance spectroscopy. Mol Biosyst 2012; 8:58-68; PMID:21874206; http://dx.doi.org/10.1039/c1mb05291h

7. Jensen MR, Markwick PRL, Meier S, Griesinger C, Zweckstetter M, Grzesiek S, et al. Quantitative determination of the conformational properties of partially folded and intrinsically disordered proteins using NMR dipolar couplings. Structure 2009; 17:1169-85; PMID:19748338; http://dx.doi.org/10.1016/j.str.2009.08.001

8. Marsh JA, Neale C, Jack FE, Choy WY, Lee AY, Crowhurst KA, et al. Improved structural characterizations of the drkN SH3 domain unfolded state suggest a compact ensemble with native-like and non-native structure. J Mol Biol 2007; 367:1494-510; PMID:17320108; http://dx.doi.org/10.1016/j.jmb.2007.01.038

9. Mohan A, Oldfield CJ, Radivojac P, Vacic V, Cortese MS, Dunker AK, et al. Analysis of molecular recognition features (MoRFs). J Mol Biol 2006; 362:1043-59; PMID:16935303; http://dx.doi.org/10.1016/j.jmb.2006.07.087

10. Garcia-Mira MM, Sadqi M, Fischer N, Sanchez-Ruiz JM, Muñoz V. Experimental identification of downhill protein folding. Science 2002; 298:2191-5; PMID:12481137; http://dx.doi.org/10.1126/science.1077809

11. Jensen MR, Communie G, Ribeiro EA Jr., Martinez N, Desfosses A, Salmon L, et al. Intrinsic disorder in measles virus nucleocapsids. Proc Natl Acad Sci U S A 2011; 108:9839-44; PMID:21613569; http://dx.doi.org/10.1073/pnas.1103270108

12. Bernadó P, Blanchard L, Timmins P, Marion D, Ruigrok RWH, Blackledge M. A structural model for unfolded proteins from residual dipolar couplings and small-angle x-ray scattering. Proc Natl Acad Sci U S A 2005; 102:17002-7; PMID:16284250; http://dx.doi.org/10.1073/pnas.0506202102

13. Hunter JD. Matplotlib: A 2D Graphics Environment. Comput Sci Eng 2007; 9:90-5; http://dx.doi.org/10.1109/MCSE.2007.55

14. Nodet G, Salmon L, Ozenne V, Meier S, Jensen MR, Blackledge M. Quantitative description of backbone conformational sampling of unfolded proteins at amino acid resolution from NMR residual dipolar couplings. J Am Chem Soc 2009; 131:17908-18; PMID:19908838; http://dx.doi.org/10.1021/ja9069024

15. Mao AH, Crick SL, Vitalis A, Chicoine CL, Pappu RV. Net charge per residue modulates conformational ensembles of intrinsically disordered proteins. Proc Natl Acad Sci U S A 2010; 107:8183-8; PMID:20404210; http://dx.doi.org/10.1073/pnas.0911107107

16. Hamelryck T, Manderick B. PDB file parser and structure class implemented in Python. Bioinformatics 2003; 19:2308-10; PMID:14630660; http://dx.doi.org/10.1093/bioinformatics/btg299

17. Cock PJA, Antao T, Chang JT, Chapman BA, Cox CJ, Dalke A, et al. Biopython: freely available Python tools for computational molecular biology and bioinformatics. Bioinformatics 2009; 25:1422-3; PMID:19304878; http://dx.doi.org/10.1093/bioinformatics/btp163

18. Frishman D, Argos P. Knowledge-based protein secondary structure assignment. Proteins 1995; 23:566-79; PMID:8749853; http://dx.doi.org/10.1002/prot.340230412

19. Irbäck A, Mitternacht S, Mohanty S. An effective all-atom potential for proteins. PMC Biophys 2009; 2:2; PMID:19356242; http://dx.doi.org/10.1186/1757-5036-2-2

20. Chakrabartty A, Ananthanarayanan VS, Hew CL. Structure-function relationships in a winter flounder antifreeze polypeptide. I. Stabilization of an α-helical antifreeze polypeptide by charged-group and hydrophobic interactions. J Biol Chem 1989; 264:11307-12; PMID:2738067

21. Maisuradze GG, Liwo A, Ołdziej S, Scheraga HA. Evidence, from simulations, of a single state with residual native structure at the thermal denaturation midpoint of a small globular protein. J Am Chem Soc 2010; 132:9444-52; PMID:20568747; http://dx.doi.org/10.1021/ja1031503

22. Fesinmeyer RM, Hudson FM, Andersen NH. Enhanced hairpin stability through loop design: the case of the protein G B1 domain hairpin. J Am Chem Soc 2004; 126:7238-43; PMID:15186161; http://dx.doi.org/10.1021/ja0379520

23. Ozenne V, Bauer F, Salmon L, Huang JR, Jensen MR, Segard S, et al. Flexible-meccano: a tool for the generation of explicit ensemble descriptions of intrinsically disordered proteins and their associated experimental observables. Bioinformatics 2012; 28:1463-70; PMID:22613562; http://dx.doi.org/10.1093/bioinformatics/bts172

24. Kjaergaard M, Nørholm AB, Hendus-Altenburger R, Pedersen SF, Poulsen FM, Kragelund BB. Temperature-dependent structural changes in intrinsically disordered proteins: formation of alpha-helices or loss of polyproline II? Protein Sci 2010; 19:1555-64; PMID:20556825; http://dx.doi.org/10.1002/pro.435

25. Krimm S, Mark JE. Conformations of polypeptides with ionized side chains of equal length. Proc Natl Acad Sci U S A 1968; 60:1122-9; PMID:16591670; http://dx.doi.org/10.1073/pnas.60.4.1122

26. Thomas AS, Elcock AH. Molecular simulations suggest protein salt bridges are uniquely suited to life at high temperatures. J Am Chem Soc 2004; 126:2208-14; PMID:14971956; http://dx.doi.org/10.1021/ja039159c

27. Wikipedia. Ramachandran Plot, http://en.wikipedia.org/wiki/Ramachandran_plot

28. Fisher CK, Stultz CM. Constructing ensembles for intrinsically disordered proteins. Curr Opin Struct Biol 2011; 21:426-31; PMID:21530234; http://dx.doi.org/10.1016/j.sbi.2011.04.001

29. Irbäck A, Mohanty S. PROFASI: A Monte Carlo simulation package for protein folding and aggregation. J Comput Chem 2006; 27:1548-55; PMID:16847934; http://dx.doi.org/10.1002/jcc.20452